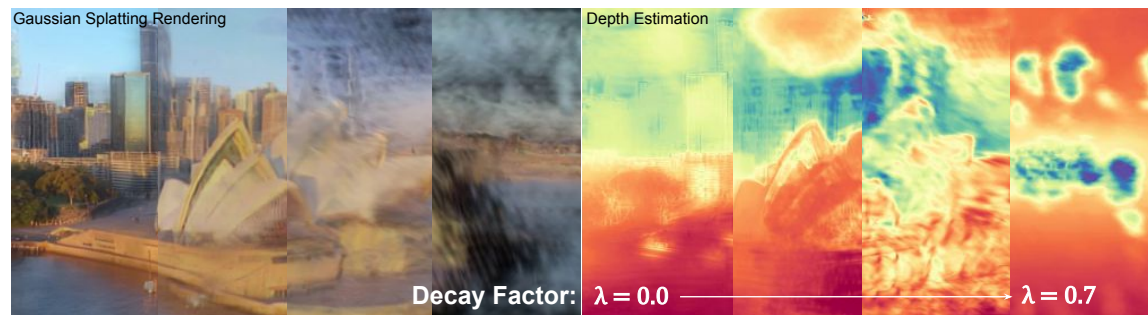


1 **Echoes of the Prior: A Computational Phenomenology of Forgetting**

2 ANONYMOUS AUTHOR(S)

3 SUBMISSION ID: ARTPL_110S1



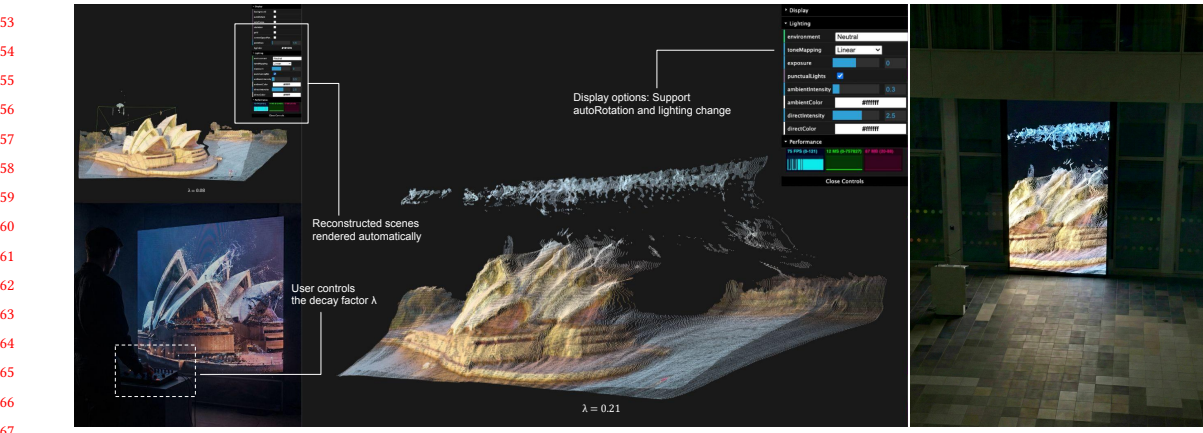


Fig. 2. **Installation Design of *Echoes of the Prior*.** Snapshot of the real-time visual feedback ($\lambda = 0.21$). The viewport displays the immediate structural dissolution of the 3D scene as the user adjusts the decay factor.

Modern Vision Transformers are rooted in biological principles of distributed representation and predictive coding. If these models functionally approximate human cognition, their pathology can simulate the pathology of the mind.

Echoes of the Prior operates on this hypothesis. We treat a state-of-the-art 3D Gaussian Splatting (3DGS) model not as a renderer, but as a conscious observer. By surgically introducing noise into its *long-term memory* (Latent Priors) and *sensory cortex* (Image Processor), we force the machine to reconstruct reality through a damaged mind. The resulting imagery – melting sky, ghostly architectures, and dissolving forms – serves as a visual translation of fading mind, making the invisible internal experience of forgetting visible, visceral, and shared.

We title our installation *DecArt* (a portmanteau of *Decay* and *Art*). Pronounced like the French philosopher *Descartes*, we elaborate on the philosophical implications of this choice in Sec. 5.1.

2 Methodology: Simulating Cognitive Decay

Modern foundational models [Oquab et al. 2024; Siméoni et al. 2025] do not store pixels; they store semantic concepts in a high-dimensional latent space. To simulate the phenomenology of forgetting, we do not merely degrade the image pixels; we perform surgical interventions on the cognitive architecture of the machine.

Our approach creates a structural homology between a state-of-the-art 3D reconstruction model [Lin et al. 2025] based on feed-forward 3D Gaussian Splatting (FF-3DGS), and the Predictive Coding framework [Friston 2010] of the human brain, synthesizing reality through the fusion of two distinct neural pathways: *memory* (prior) and *evidence* (sensation).

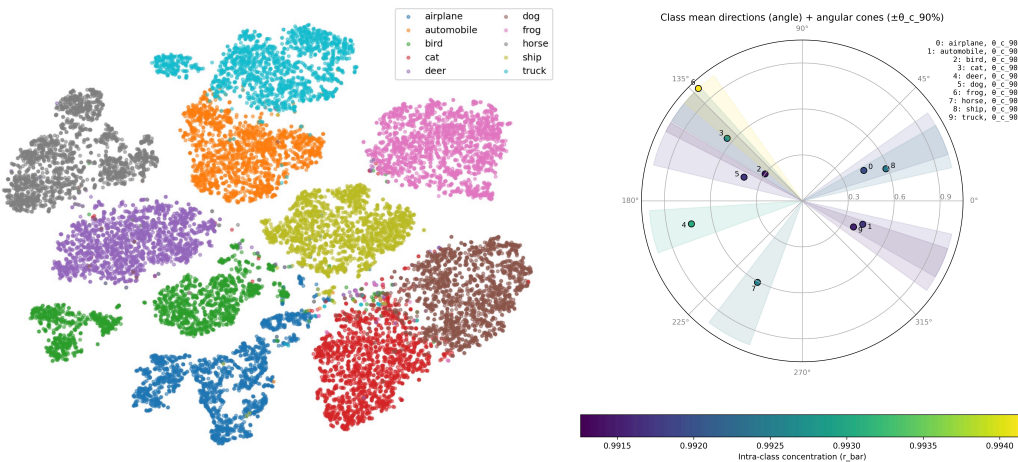
2.1 The Silicon Proxy: Two Streams Mapping Mind to Code

Can a machine possess memory and cognition? If so, what does it look like?

The act of perceiving the world is a negotiation between what our eyes see – the evidence from *Sensory Cortex*, and what our brains expect – the *Engram* which refers to the physical trace of memory in neuroscience. We map this biological duality onto the specific components of our computational architecture:

105 2.1.1 *The Sensory Stream: Processor Weights.* Mirroring the biological retina and V1 cortex, our model employs a
 106 shallow CNN to process raw pixel inputs, capturing the texture and local geometry of the *Now*. This sensory signal will
 107 serve as a reinforcement to the memory, and together with memory, will be injected into a fusion block for spatial
 108 perception and reconstruction [Ranftl et al. 2021].
 109

110
 111 2.1.2 *The Memory Stream: Semantic Features.* Just as biological memory stores concepts rather than raw data, our
 112 system utilizes vision foundational models to encode high-dimensional semantic priors.
 113



131
 132 Fig. 3. t-SNE visualization of the DINOv2 latent space. **(Left)** Semantic concepts cluster into distinct manifolds, representing the
 133 structured *healthy* memory baseline. **(Right)** Cosine similarity metrics confirm that intra-class features are more closely aligned than
 134 inter-class features, validating the semantic coherence of the latent space.
 135
 136

137 Specifically, we use **DINOv2** [Oquab et al. 2024], a state-of-the-art visual understanding model as the *prior* producer in
 138 our feed-forward 3D reconstruction model. To give an intuitive sense of this prior, we visualize its latent representation
 139 space. As shown in Fig. 3 on the left, in this high-dimensional (1024D) latent space, for instance, visual features of the
 140 same semantic concept cluster together and form a distinct manifold, diverging significantly from others in terms of
 141 geometric similarity metrics. We employ t-SNE and PCA to project these 1024D latent vectors into 2D space for better
 142 visualization. These latent representations serve as the *healthy baseline*: the long-term memory of a healthy silicon
 143 brain – structured, dense, and semantically coherent.
 144

145
 146 In a healthy state, perception is the successful integration of these two streams. Our installation visualizes what
 147 happens when these streams decay asynchronously.
 148

149 2.2 The Mechanics of Forgetting: Two Decay Functions Simulating Biological Entropy

150
 151 Human aging is characterized by two distinct processes: sensory degradation and cognitive decline. To simulate both
 152 processes, we introduce two distinct entropy operators, G_{sense} and F_{mem} , grounded in the *Neural Gain Theory of*
 153 *Aging* [Li et al. 2001], which posits that both types of degradation are driven by a reduction in the signal-to-noise ratio
 154 within specific neuromodulatory systems.
 155

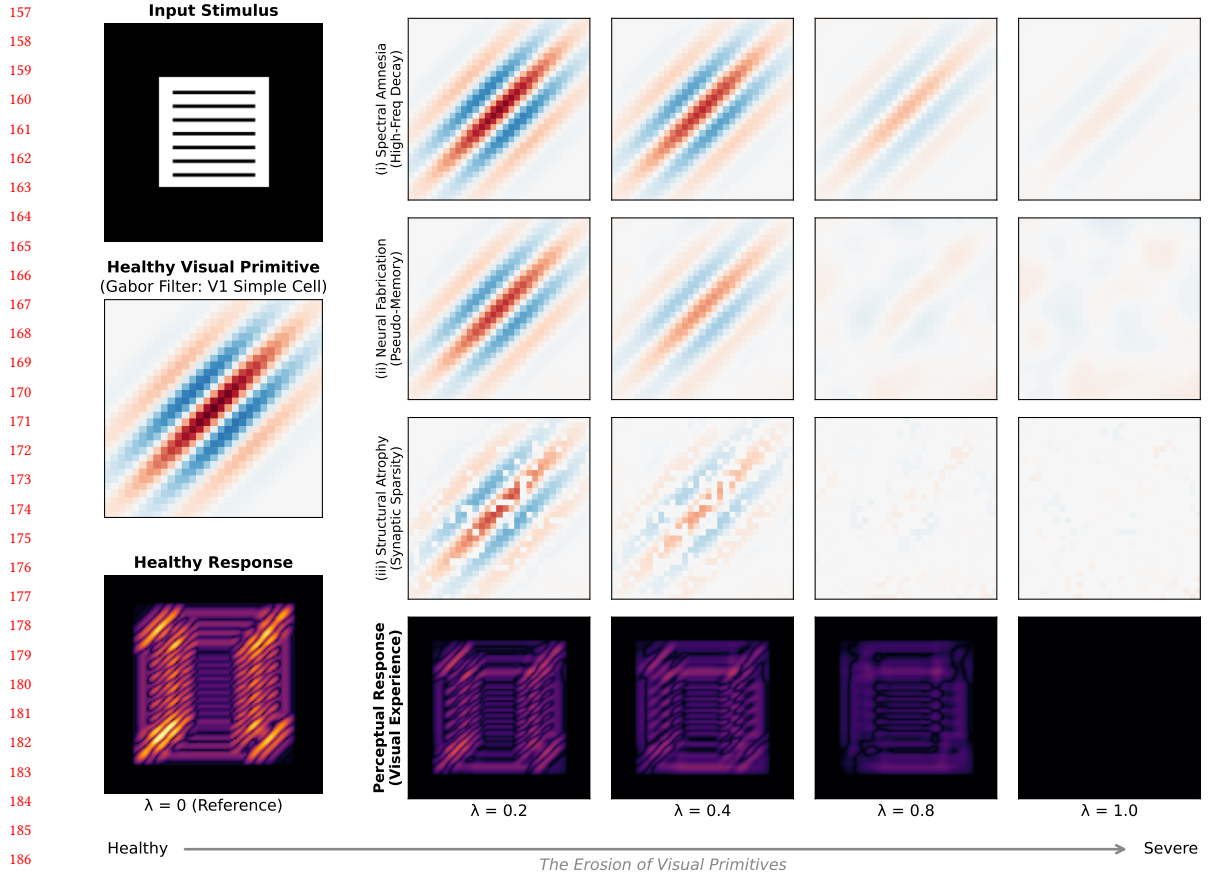


Fig. 4. Simulating Sensory Decay $\mathcal{G}_{\text{sense}}$. **(Left) Healthy Baseline ($\lambda = 0$):** Response of a standard Gabor filter (V1 primitive) to a sharp stimulus. **(Right) Pathology:** As λ increases, the filter degrades via three mechanisms: **(i) Spectral Amnesia** (loss of high-frequency acuity/sharpness); **(ii) Neural Fabrication** (injection of coherent noise/hallucinations); and **(iii) Structural Atrophy** (synaptic sparsity leading to signal loss).

2.2.1 Sensory Decay: The Erosion of Visual Primitives \mathcal{G}_{sense} . While the semantic stream deals with concepts, the sensory stream deals with *visual primitives* – edges, textures, and local gradients. A naive simulation of sensory decay would simply degrade the input signal (i.e., pixel-level corruptions), simulating external visual impairments. However, biological aging is a neurological process where the processing circuitry itself degrades.

To simulate this, we perform a perturbation on the CNN weights that acts as the machine’s primary visual cortex (as described in Sec. 2.1.1). We implement a compound decay function G_{sense} that creates a diseased clone of the sensory encoder, modeling three distinct biological failures:

(i) Spectral Amnesia (High-Frequency Domain Decay): Biological aging often begins with the loss of high-frequency acuity [Owsley et al. 1983]. To simulate this, we transform the convolutional kernels into the frequency domain via Fast Fourier Transform (FFT) and then apply a radial mask that selectively dampens high-frequency components relative to

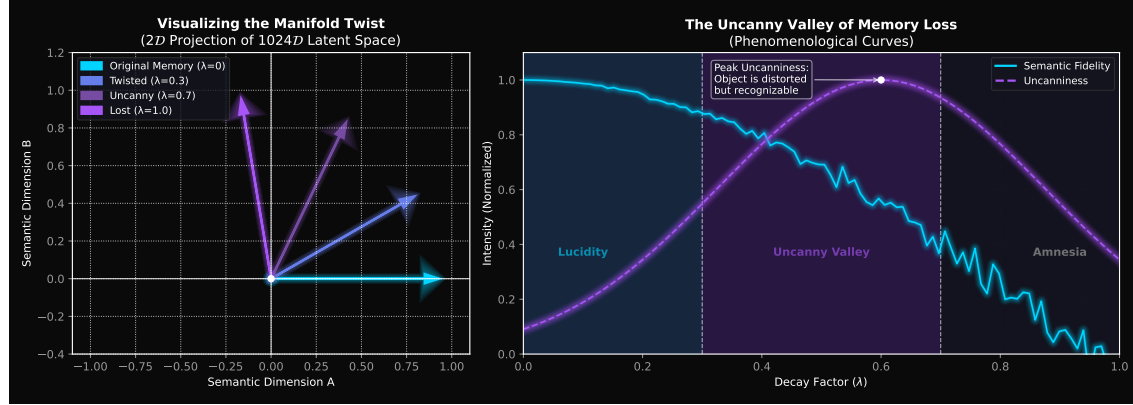


Fig. 5. **Topology of Memory Decay.** (a) **Manifold Twist:** Visualization of the orthogonal rotation $R(\lambda)$. As λ increases (blue → purple), the feature vector rotates away from its semantic alignment while preserving its norm. (b) **Uncanny Valley:** A conceptual model of visual *Uncanniness* (purple), defined as the product of structural integrity (norm) and semantic distortion ($1 - \cosine \text{ similarity}$). The peak ($0.3 < \lambda < 0.7$) corresponds to the zone where the representation is structurally strong yet semantically twisted, producing the most disturbing visual artifacts before fading into incoherent noise.

the decay factor λ ¹. This operation is grounded in the functional architecture of the primary visual cortex (V1), where simple cells act as spatiotemporal frequency filters [De Valois et al. 1982]. By dampening high frequencies in the kernel weights directly, rather than the input image, we simulate the degradation of the neurons' receptive fields themselves, rendering them incapable of resonating with fine details. **The Effect:** As shown in Fig. 4, the machine does not see a blurry image; it simply forgets how to detect sharpness. The neural filters responsible for recognizing crisp edges and fine textures (modeled as Gabor-like simple cells [Hubel and Wiesel 1962]) are chemically suppressed, simulating the onset of cortical cataracts.

(ii) **Neural Fabrication (Pseudo-Memory Injection):** The brain abhors a sensory vacuum. When visual inputs degrade, the visual cortex often generates spontaneous activity to fill the void (e.g., Charles Bonnet Syndrome [Reichert et al. 2013]). We model this by injecting spatially smoothed Gaussian noise into the weights. This approximates the “correlated noise” observed in neural circuits when inhibitory control weakens [Shadlen and Newsome 1998]. Unlike white noise, this smooth noise creates coherent but fictitious patterns in the convolution filters. **The Effect:** This causes the machine to *hallucinate* textures that do not exist, overlaying the real world with a dream-like, phantom grain.

(iii) **Structural Atrophy (Synaptic Sparsity):** Finally, we simulate the physical death of neurons. We apply a stochastic mask to the *Weight* matrix, zeroing out connections based on λ . Simultaneously, the *Bias* terms in the convolutional layers are decayed towards zero, representing a loss of neural “confidence” or activation potential. **The Effect:** This creates a *sparse* perception and the image becomes *ghostly*. As the machine loses the confidence to assert the existence of matter, the reconstructed 3D world becomes translucent and ethereal, creating a visual metaphor for a consciousness that is slowly detaching from physical reality.

2.2.2 *Memory Decay: Manifold Distortion and Cognitive Entropy \mathcal{F}_{mem}* . Biological forgetting is often a structural collapse of meaning, where the world does not just fade into black but turns disturbingly wrong. To simulate the phenomenology of *Semantic Dementia* [Warrington 1975] and *Associative Agnosia* [Farah 2004], we model the machine

¹The decay factor in $\mathcal{G}_{\text{sense}}$ can be distinct from the one in memory decay \mathcal{F}_{mem} for asynchronous control, and we keep the same symbols here to avoid complicating the notation.

memory as a high-dimensional vector field (as introduced in Sec 2.1.2), where the semantic identity of an object is defined mainly by the direction of its **feature vector** \mathbf{z} [Wang and Isola 2020], and introduce a *geometric perturbation* within the high-dimensional memory space.

The Distortion: We model *cognitive decline* acts as a force that *twists* the memory manifold. Using a continuous orthogonal rotation $\mathbf{R}(\lambda)$, we misalign semantic vectors while preserving their norm:

$$\mathbf{R}(\lambda) = (1 - \lambda) \cdot \mathbf{I} + \lambda \cdot \mathbf{Q}, \quad (1)$$

where \mathbf{Q} is a random orthogonal matrix generated via QR decomposition [Mezzadri 2007], \mathbf{I} is the identity matrix. As the decay factor λ increases, the semantic feature vectors \mathbf{z} are smoothly rotated away from their ground truth alignment.

$$\mathbf{z}_{\text{rot}} = \mathbf{z} \cdot \mathbf{R}(\lambda)^T. \quad (2)$$

This simulates a brain state where neural firing rates (signal strength) remain high, but the semantic connectivity (signal direction) is twisted – suffering from “cognitive confusion”. The machine continues to reconstruct complex, high-confidence geometries, but because the vectors are misaligned with the original priors, familiar objects are rendered as *hallucinated* topological variants. For instance, as shown in Fig. 1, a construction might be reconstructed with similar texture but the geometry of a liquid.

The Hybrid Entropy: Furthermore, to capture the full spectrum of memory decay, we combine this geometric twisting with a secondary entropy term, reflecting the irreversible loss of information:

$$\mathcal{F}_{\text{mem}}(\mathbf{z}, \lambda, \gamma) = \underbrace{(1 - \gamma) \cdot \mathbf{z}_{\text{rot}}}_{\text{Distortion}} + \underbrace{\gamma \cdot \mathcal{N}(\mathbf{z})}_{\text{Entropy}} \quad (3)$$

where $\mathbf{z}, \mathbf{z}_{\text{rot}} \in \mathbb{R}^D$ are feature vectors (here $D = 1024$), function $\mathcal{N}(\mathbf{z})$ generates a stochastic noise vector, $\mathcal{N}(\mathbf{z}) \approx \epsilon \cdot \|\mathbf{z}\|$, where $\epsilon \sim \mathcal{N}(0, I)$. By fusing manifold rotation ($1 - \gamma = 0.7$) with stochastic noise ($\gamma = 0.3$), the system visualizes a specific trajectory of forgetting: as shown in Fig. 5, memory first becomes confused (twisted geometry) before it eventually becomes lost (dissolved form). This algorithmic choice allows us to visualize the *uncanny valley* of memory loss, mirroring the phenomenology of Associative Agnosia [Farah 2004] and Semantic Dementia [Warrington 1975], where the patient perceives form without meaning.

2.3 The Selective Forgetting: Object-Oriented Amnesia

While global decay simulates a systemic cognitive decline (e.g., dementia), human forgetting is often highly selective [Warrington 1975]. We frequently lose the semantic grasp of specific entities – a face, a name, or an object – while the surrounding reality remains intact. To simulate this *dissociative amnesia*, we introduce a targeted decay mechanism that allows the system to surgically erode the memory of specific semantic categories.

2.3.1 Semantic Grounding and Masking. We employ a two-stage pipeline to isolate the *memory trace* of a specific object. First, we utilize an open-vocabulary detection model, **Grounded-SAM** [Ren et al. 2024], to generate a pixel-level binary mask $M_{\text{pixel}} \in \{0, 1\}$ based on a textual prompt (e.g., “woman in red”). This mask represents the object’s footprint in the visual field. As shown in Fig. 6, users can obtain the mask for specific entities by providing a text prompt or drawing bounding boxes. A naive approach would be to apply the mask to the input image directly (pixel-level inpainting), but this would result in a superficial “black hole” rather than a cognitive loss. Instead, we perform the intervention within the latent feature space of the memory.

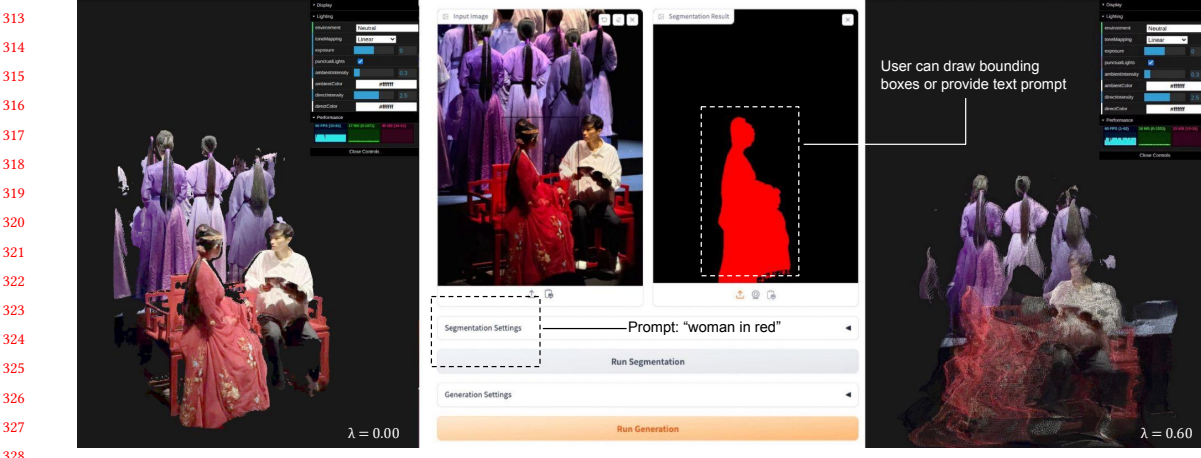


Fig. 6. **Visualizing Selective Forgetting.** Targeted entropy injection using a text prompt ("woman in red"). (**Left**) Original reconstruction. (**Right**) Decayed result ($\lambda = 0.6$). The targeted entity undergoes topological dissolution, effectively ghosting out of reality while the surrounding context remains intact.

2.3.2 *Latent Space Surgery*. To extract the prior about the input images, the vision foundation model [Oquab et al. 2024] first processes images as a sequence of patch tokens. To align with the spatial shape of these patch tokens, we down-sample the pixel mask M_{pixel} to create a discretized token-wise mask $M_{\text{token}} \in \{0, 1\}$.

We then modify the forward pass of our system: we perform decay function Eq. (3) only into the tokens corresponding to the target object:

$$\mathbf{z}' = M_{\text{token}} \cdot \mathcal{F}_{\text{mem}}(\mathbf{z}, \lambda, \gamma) + (1 - M_{\text{token}}) \cdot \mathbf{z}, \quad (4)$$

where \mathbf{z} is the original clear memory.

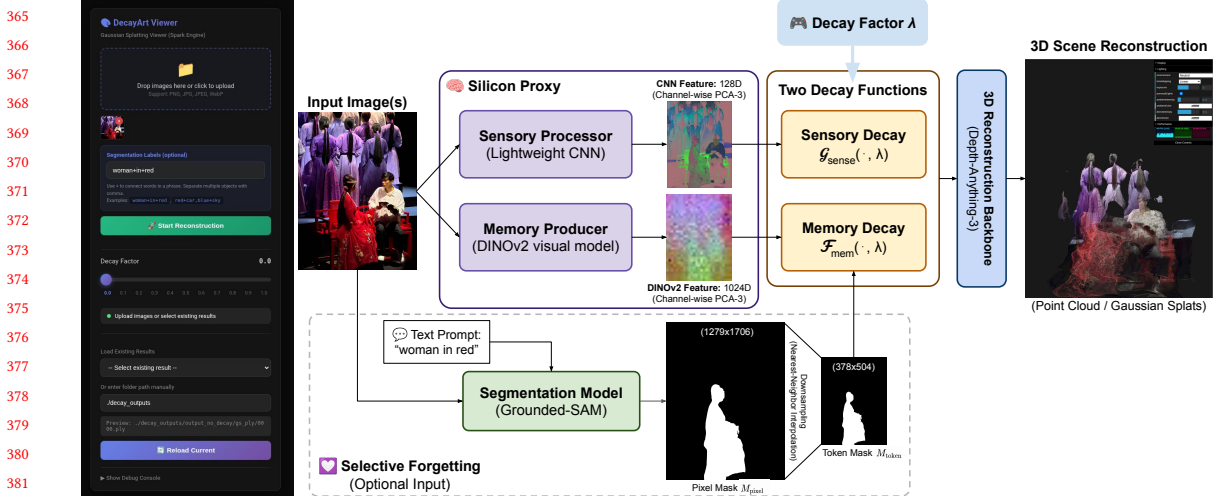
By perturbing only the latent tokens of the target, we achieve a form of *selective agnosia*. As shown in Fig. 6 on the right, the reconstructed 3D point cloud of the surrounding environment (e.g., other actors) remains structurally sound. However, the targeted entity (e.g., "woman in red") begins to exhibit a topological failure: its geometry melts, its texture turns into noise, and it effectively ghosts out of physical existence. This visualizes the psychological state where a patient may perceive the context of a room perfectly but fails to resolve the identity or form of a specific object within it – a computational emulation of the brain's refusal to process a traumatic memory. We give more discussion in Sec 5.3.

3 Real-time Installation and Implementation Details

3.1 User Interface and Integration Formula

We designed *Echoes of the Prior* as a real-time interactive installation. The core of the installation is a closed-loop reconstruction system that processes visual stimuli into decaying 3D memories.

As shown in Fig. 7, the system accepts visual input (either from a live camera feed capturing the viewer's environment or pre-loaded image dataset) and processes it through a pre-trained 3D reconstruction backbone, **Depth Anything 3** [Lin et al. 2025], for memory construction. Unlike standard inference, the user-defined decay factor λ intercepts this reconstruction process by two parallel decay functions: **The Sensory Decay Path (Top)**, which acts as a spectral filter (see Sec. 2.2.1); **The Memory Decay Path (Bottom)**, which optionally integrates a **Selective Forgetting** module. This module utilizes **Grounded-SAM** [Ren et al. 2024] to generate semantic masks based on user prompts. Entropy

Fig. 7. The System Workflow of *Echoes of the Prior*.

is **surgically injected** only into the tokens representing specific objects, disrupting their structural integrity while preserving the context. Finally, these corrupted latents from both paths are fused together and then decoded by the 3D reconstruction backbone into a fractured 3D scene represented by Gaussian Splats or point cloud, which is rendered in real-time via a WebGL-based viewer to provide immediate visual feedback of the decay. The system supports 60FPS interaction: as the user slides the fader, the world melts instantly, creating a visceral connection between their action and the visual destruction.

Designed with minimalist semantics, the interface centers on a single slider ($\lambda \in [0, 1]$). This transforms an abstract algorithm into a proprioceptive experience: as the user physically drags the fader, they witness the immediate entropic dissolution of the scene. Unlike static video loops, the rendered scene supports full orbit controls. Users can rotate and zoom into the decaying structures, inspecting the glitch artifacts up close.

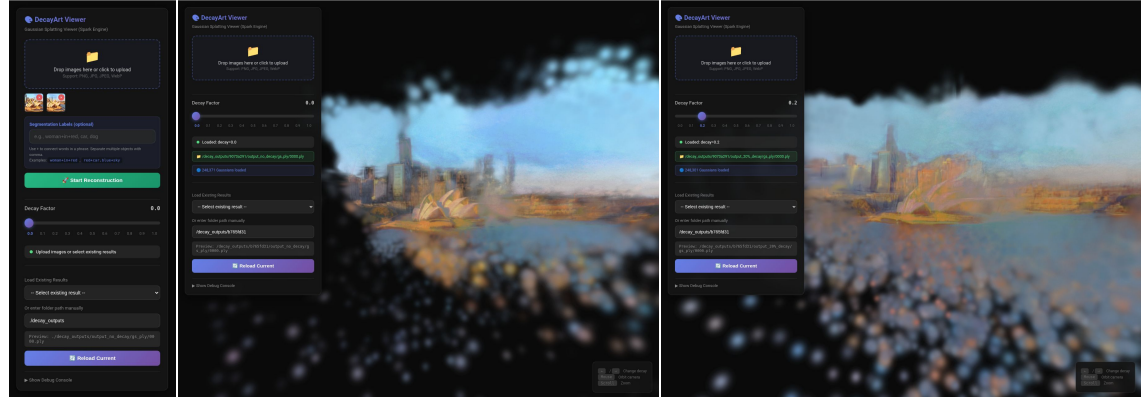


Fig. 8. The Interactive Interface. The web-based GUI enables real-time interaction with the decay process.

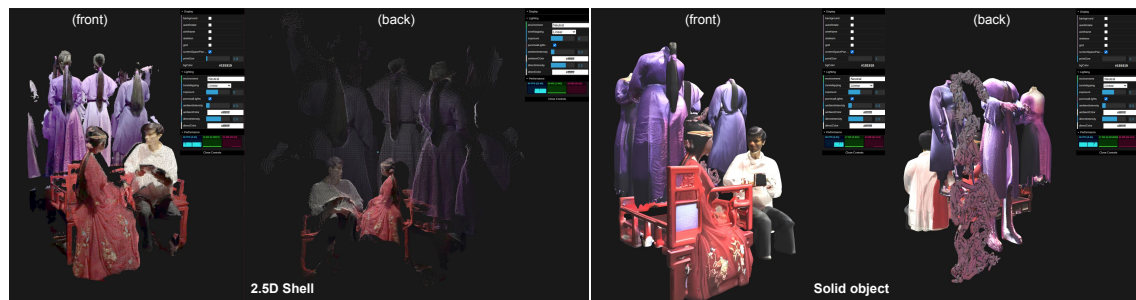
417 3.2 Image Acquisition Strategy

418 The system supports dual inputs: a **Curated Archive** of semantic archetypes for immediate engagement, and a **Personal**
 419 **Injection** feature allowing users to upload personal photos or video, transforming the installation into a digital elegy.

420 While the paper figures illustrate the core algorithm, we developed an advanced **Interactive Streaming Interface**
 421 (shown in the demo video, a representative frame shown in Fig. 10) to facilitate real-time experimentation. This system
 422 integrates Grounded-SAM for prompt-based masking and implements a batch pre-computation pipeline, allowing users
 423 to seamlessly visualize the continuous decay process in 4D space without inference latency.

427 3.3 Negative Justification: The Ontology of the Shell

428 In the development of *Echoes of the Prior*, we evaluated two distinct paradigms for 3D scene reconstruction: (1) generative
 429 multi-view diffusion, represented by MIDI-3D [Huang et al. 2025], and (2) monocular depth reconstruction, represented
 430 by Depth Anything V3 (DA3) [Lin et al. 2025].



444 **Fig. 9. Memory as a Potemkin Village: Hallucination vs. Reconstruction.** While 3D generative models (**Right**) fabricate a
 445 complete, watertight object by inventing unseen details, our system (**Left**) preserves the epistemological honesty of the input. It
 446 projects a thin, fragile film, like a *façade* of memory, that disintegrates when the viewer attempts to look behind the veil. This
 447 hollowness is not a technical failure, but a deliberate aesthetic feature representing the void of forgotten context.

450 While generative models offer watertight meshes, we find such completeness antithetical to memory. Memory is
 451 a surface, not a solid [Merleau-Ponty 1945]. We therefore choose DA3’s monocular reconstruction to preserve the
 452 *Potemkin village effect*: a fragile film that reveals its void upon rotation, metaphorically representing the emptiness of
 453 forgotten contexts.

455 4 Related Work

456 Positioning *Echoes of the Prior* requires navigating the intersection of three distinct disciplines: computational aesthetics,
 457 volumetric computer vision, and theoretical neuroscience.

460 4.1 From Machine Vision to Machine Hallucination

461 In the domain of AI art, early works focused on visualizing the *constructive* capacity of neural networks. **Deep-**
 462 **Dream** [Mordvintsev et al. 2015] and **Neural Style Transfer** [Gatys et al. 2016] exposed the internal representations
 463 of CNNs by maximizing feature activation, essentially asking the machine to “see more” of what it knows. Contempo-
 464 **rary media artists like Refik Anadol** [Anadol 2021] have further expanded this by treating massive datasets as fluid
 465 memories, visualizing the *learning* process of the machine.

469 Our work inverts this paradigm. Instead of visualizing the *genesis* of intelligence (learning), we visualize its *entropy*
 470 (forgetting). We align with the tradition of **Glitch Art** [Menkman 2011], which views technological failure not as a bug,
 471 but as a revelation of the underlying medium. However, unlike traditional glitches that operate on the surface pixel
 472 level (e.g., datamoshing), our system performs **structural pathology**: we erode the internal cognitive weights and
 473 predictive priors themselves. This creates a form of “Deep Glitch” that emulates neurodegeneration rather than mere
 474 signal transmission error.
 475

477

478

4.2 Spatializing the Past: 3D Reconstruction as a Cognitive Medium

479

480 While photography freezes a specific moment (a temporal slice), 3D reconstruction captures a specific environment
 481 (a spatial slice). We argue that **volumetric 3D representation** is intrinsically more akin to the phenomenology of
 482 biological memory than flat 2D imagery. Neuroscientific evidence suggests that memory encoding is deeply intertwined
 483 with spatial navigation (e.g., in the hippocampus) [O’Keefe and Dostrovsky 1971]. To remember is not just to view an
 484 image; it is to inhabit a space.

485

486 The evolution of 3D reconstruction, from explicit photogrammetry meshes to implicit **Neural Radiance Fields**
 487 (**NeRF**) [Mildenhall et al. 2020] and now **3D Gaussian Splatting (3DGS)** [Kerbl et al. 2023], reflects a shift towards
 488 more organic representations of reality. Unlike polygonal meshes which are defined by rigid surfaces, volumetric
 489 approaches represent the world as a probabilistic field of density and color.

490

491 In this work, we utilize 3DGS as our implementation carrier not merely for its real-time rendering capabilities, but for
 492 its unique aesthetic properties. Unlike generative video models that hallucinate temporal continuity, 3DGS reconstructs
 493 the *spatial continuity* of a scene. By subjecting this volumetric representation to decay, we visualize the disintegration
 494 of the spatial context itself, simulating how a patient might lose their grip on the *where* and *how* of a memory, rather
 495 than just the *what*.

496

497

4.3 Computational Psychiatry and Predictive Coding

498

499 Theoretically, our decay functions are grounded in the **Free Energy Principle** [Friston 2010], which posits that the brain
 500 minimizes surprise by constantly predicting sensory input based on internal priors. In this framework, psychopathology
 501 is often modeled as a failure of this predictive machinery [Corlett et al. 2019].

502

503 Our implementation of the Sensory Decay ($\mathcal{G}_{\text{sense}}$) draws directly from the **Neural Gain Theory of Aging** [Li
 504 et al. 2001], which hypothesizes that cognitive decline is driven by a reduction in the signal-to-noise ratio (SNR) of
 505 neuromodulators (like dopamine) in the cortex. By injecting noise into the weights of our vision encoder, we create a
 506 functional homology of this biological process. Furthermore, our simulation of hallucinations aligns with models of
 507 **Computational Psychiatry**, which suggest that when sensory precision is low (as in our Spectral Amnesia module),
 508 the brain over-relied on top-down priors, leading to the perception of phantom stimuli [Powers et al. 2017].

509

510 Complementing this, our Memory Decay (\mathcal{F}_{mem}) simulates the breakdown of top-down priors, grounded in the
 511 theory of **Attractor Dynamics** [Hopfield 1982]. In biological networks, memories are stored as stable states (attractors)
 512 within a high-dimensional manifold. Our geometric rotation of the latent space effectively destabilizes these attractors,
 513 simulating the phenomenology of **Semantic Dementia** [Warrington 1975], a condition where the structural links
 514 between concepts erode. While the machine retains the raw sensory data, it loses the “semantic glue” that holds the
 515 geometry together, mirroring how patients with associative agnosia perceive form without meaning.

516

517 Manuscript submitted to ACM

518

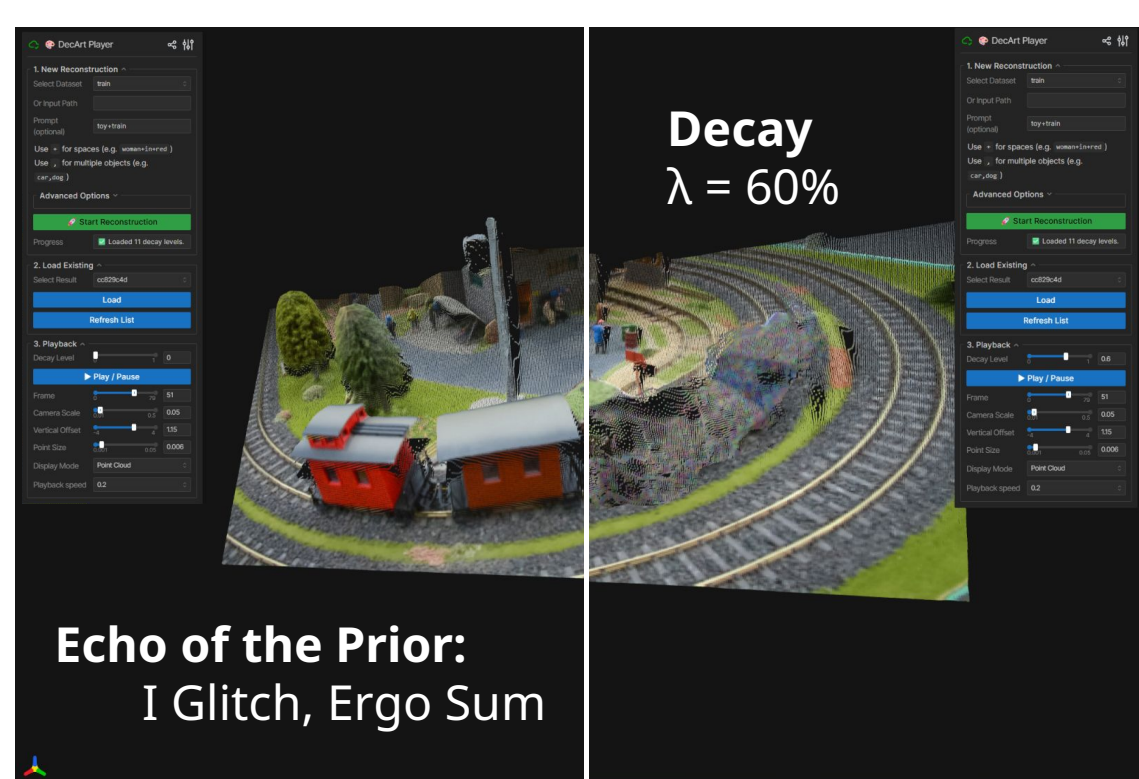
519

520

521 **5 Discussion and Future Work**

522 **5.1 Design Insights: Glitcho, Ergo Sum**

523 The homophone *DecArt* invites a reflection on *Cartesian doubt* in the age of silicon. Descartes famously stripped away
 524 all sensory perception as potentially deceptive, arriving at the only undeniable truth: *Cogito, Ergo Sum* (I think, therefore
 525 I am). Our installation poses a parallel question for the machine: when the sensory weights rot and the semantic priors
 526 twist, does the “ghost in the shell” still exist? Or, in our case: *Glitcho, Ergo Sum* (I glitch, therefore I am).



557 Fig. 10. “**I Glitch, Ergo Sum**” (**I glitch, therefore I am**). A visual manifesto generated by our real-time streaming system **DecArt**.

559 This suggests a profound irony: a perfectly optimized neural network is merely a sterile photocopier – accurate, yet
 560 alien. The “humanity” of the machine emerges not in its computation, but in its poetic failure. When the AI struggles to
 561 reconstruct reality from corrupted memory, it ceases to be a tool and becomes a mirror, forcing the audience to confront
 562 the inevitability of their own cognitive entropy. Ultimately, we argue that generative AI can be more than an engine for
 563 productivity; it can be a medium for *radical empathy*.

566 **5.2 Limitation: The Gap between Simulation and Sensation**

568 While we successfully simulate the visual phenomenology of memory loss (the *look* of forgetting), we cannot simulate
 569 the affective sensation (the *feeling* of sadness). The machine does not miss the objects it forgets; it simply processes noise.
 570 This highlights the *Hard Problem of Consciousness* [Chalmers 1995]. Our system is a *Functionalism* model of amnesia, not
 571

573 a phenomenological one. Future work could integrate *Affective Computing* modules to modulate the decay based on a
 574 simulated *emotional state* of the AI.
 575

576 577 5.3 Artifacts in Selective Forgetting: The Impossibility of Clean Forgetting

578 Our current implementation of object-aware forgetting relies on mapping pixel-level segmentation masks to the lower-
 579 resolution latent space of the memory. The necessary down-sampling and interpolation of the binary masks result in
 580 imperfect alignment at object boundaries, leading to a halo effect where the decay noise spills over into adjacent pixels.
 581 While technically a precision error, this limitation may align with the project's conceptual framework. It visualizes
 582 the impossibility of isolating a single memory trace without affecting its connected reality – the impossibility of *clean*
 583 *forgetting*. Just as a fading memory often blurs the details of its spatial context, our installation's inability to perform a
 584 clean cut reflects the entangled nature of visual perception.
 585

586 587 5.4 Future Work: Towards a Romantic Neuromorphic Art

588 While standard Artificial Neural Networks (ANNs) constitute the backbone of current AGI, they represent a static
 589 “snapshot” of thought. To simulate *living* memory, we aim to transition to Spiking Neural Networks (SNNs) [Maass
 590 1997]. Though currently confined to neuromorphic robotics, we repurpose this event-driven technology to visualize the
 591 *silencing of time*, where forgetting is not just noise, but the cessation of firing.
 592

593 594 References

- 595 Refik Anadol. 2021. Machine Hallucinations. Exhibition at Pilevneli Gallery, Istanbul.
- 596 David J Chalmers. 1995. Facing up to the problem of consciousness. *Journal of Consciousness Studies* 2, 3 (1995), 200–219.
- 597 Philip R Corlett, Guillermo Horga, Paul C Fletcher, Ben Alderson-Day, Katharina Schmack, and Albert R Powers. 2019. Hallucinations and strong priors. *Trends in cognitive sciences* 23, 2 (2019), 114–127.
- 598 Russell L De Valois, Duane G Albrecht, and Lisa G Thorell. 1982. Spatial frequency selectivity of cells in macaque visual cortex. *Vision research* 22, 5 (1982), 545–559.
- 599 Martha J Farah. 2004. *Visual Agnosia*. MIT Press.
- 600 Karl Friston. 2010. The free-energy principle: a unified brain theory? *Nature reviews neuroscience* 11, 2 (2010), 127–138.
- 601 Leon A Gatys, Alexander S Ecker, and Matthias Bethge. 2016. Image style transfer using convolutional neural networks. In *Proceedings of the IEEE conference on computer vision and pattern recognition (CVPR)*. 2414–2423.
- 602 John J Hopfield. 1982. Neural networks and physical systems with emergent collective computational abilities. *Proceedings of the National Academy of Sciences* 79, 8 (1982), 2554–2558.
- 603 Zehuan Huang, Yuan-Chen Guo, Xingqiao An, Yunhan Yang, Yangguang Li, Zi-Xin Zou, Ding Liang, Xihui Liu, Yan-Pei Cao, and Lu Sheng. 2025. Midi: Multi-instance diffusion for single image to 3d scene generation. In *Proceedings of the Computer Vision and Pattern Recognition Conference*. 23646–23657.
- 604 David H Hubel and Torsten N Wiesel. 1962. Receptive fields, binocular interaction and functional architecture in the cat's visual cortex. *The Journal of Physiology* 160, 1 (1962), 106–154.
- 605 Bernhard Kerbl, Georgios Kopanas, Thomas Leimkühler, and George Drettakis. 2023. 3d gaussian splatting for real-time radiance field rendering. *ACM Transactions on Graphics (TOG)* 42, 4 (2023), 1–14. SIGGRAPH 2023.
- 606 Shu-Chen Li, Ulman Lindenberger, and Sverker Sikström. 2001. Aging cognition: from neuromodulation to representation. *Trends in cognitive sciences* 5, 11 (2001), 479–486.
- 607 Haotong Lin, Sili Chen, Junhao Liew, Donny Y. Chen, Zhenyu Li, Guang Shi, Jiashi Feng, and Bingyi Kang. 2025. Depth Anything 3: Recovering the Visual Space from Any Views. arXiv:2511.10647 [cs.CV]
- 608 Wolfgang Maass. 1997. Networks of spiking neurons: The third generation of neural network models. *Neural networks* 10, 9 (1997), 1659–1671.
- 609 Rosa Menkman. 2011. *The glitch moment(um)*. Institute of Network Cultures.
- 610 Maurice Merleau-Ponty. 1945. *Phenomenology of Perception*. Gallimard.
- 611 Francesco Mezzadri. 2007. How to generate random matrices from the classical compact groups. *Notices of the AMS* 54, 5 (2007), 592–604.
- 612 Ben Mildenhall, Pratul P Srinivasan, Matthew Tancik, Jonathan T Barron, Ravi Ramamoorthi, and Ren Ng. 2020. Nerf: Representing scenes as neural radiance fields for view synthesis. In *European conference on computer vision (ECCV)*. 405–421.
- 613 Alexander Mordvintsev, Christopher Olah, and Mike Tyka. 2015. Inceptionism: Going deeper into neural networks. *Google Research Blog* (2015).
- 614 615 Manuscript submitted to ACM

- 625 John O'Keefe and Jonathan Dostrovsky. 1971. The hippocampus as a spatial map: preliminary evidence from unit activity in the freely-moving rat. *Brain research* 34, 1 (1971), 171–175. Nobel Prize winning work on Place Cells.
- 626
- 627 Maxime Oquab, Timothée Darcet, Théo Moutakanni, Huy V. Vo, Marc Szafraniec, Vasil Khalidov, Pierre Fernandez, Daniel HAZIZA, Francisco Massa,
- 628 Alaaeldin El-Nouby, Mido Assran, Nicolas Ballas, Wojciech Galuba, Russell Howes, Po-Yao Huang, Shang-Wen Li, Ishan Misra, Michael Rabbat, Vasu
- 629 Sharma, Gabriel Synnaeve, Hu Xu, Herve Jegou, Julien Mairal, Patrick Labatut, Armand Joulin, and Piotr Bojanowski. 2024. DINoV2: Learning Robust
- 630 Visual Features without Supervision. *Transactions on Machine Learning Research* (2024).
- 631 Cynthia Owsley, Robert Sekuler, and Dennis Siemsen. 1983. Contrast sensitivity throughout adulthood. *Vision Research* 23, 7 (1983), 689–699.
- 632 Albert R Powers, Christoph Mathys, and Philip R Corlett. 2017. Pavlovian conditioning-induced hallucinations result from overweighting of perceptual
- 633 priors. *Science* 357, 6351 (2017), 596–600.
- 634 René Ranftl, Alexey Bochkovskiy, and Vladlen Koltun. 2021. Vision transformers for dense prediction. In *Proceedings of the IEEE/CVF international*
- 635 *conference on computer vision (ICCV)*. 12179–12188.
- 636 David P Reichert, Peggy Seriès, and Amos J Storkey. 2013. Charles Bonnet Syndrome: Evidence for a Generative Model in the Cortex? *PLOS Computational*
- 637 *Biology* 9, 7 (2013), e1003134.
- 638 Tianhe Ren, Shilong Liu, Ailing Zeng, Jing Lin, Kunchang Li, He Cao, Jiayu Chen, Xinyu Huang, Yukang Chen, Feng Yan, Zhaoyang Zeng, Hao Zhang,
- 639 Feng Li, Jie Yang, Hongyang Li, Qing Jiang, and Lei Zhang. 2024. Grounded SAM: Assembling Open-World Models for Diverse Visual Tasks.
- 640 arXiv:2401.14159 [cs.CV]
- 641 Michael N Shadlen and William T Newsome. 1998. The Variable Discharge of Cortical Neurons: Implications for Connectivity, Computation, and
- 642 Information Coding. *Journal of Neuroscience* 18, 10 (1998), 3870–3896.
- 643 Oriane Siméoni, Huy V. Vo, Maximilian Seitzer, Federico Baldassarre, Maxime Oquab, Cijo Jose, Vasil Khalidov, Marc Szafraniec, Seungeun Yi, Michaël
- 644 Ramamonjisoa, Francisco Massa, Daniel Haziza, Luca Wehrstedt, Jianyuan Wang, Timothée Darcet, Théo Moutakanni, Leonel Santana, Claire Roberts,
- 645 Andrea Vedaldi, Jamie Tolan, John Brandt, Camille Couprie, Julien Mairal, Hervé Jégou, Patrick Labatut, and Piotr Bojanowski. 2025. DINoV3.
- 646 arXiv:2508.10104 [cs.CV] <https://arxiv.org/abs/2508.10104>
- 647 Tongzhou Wang and Phillip Isola. 2020. Understanding Contrastive Representation Learning through Alignment and Uniformity on the Hypersphere. In
- 648 *International Conference on Machine Learning (ICML)*. PMLR, 9929–9939.
- 649 Elizabeth K Warrington. 1975. The selective impairment of semantic memory. *The Quarterly Journal of Experimental Psychology* 27, 4 (1975), 635–657.
- 650
- 651
- 652
- 653
- 654
- 655
- 656
- 657
- 658
- 659
- 660
- 661
- 662
- 663
- 664
- 665
- 666
- 667
- 668
- 669
- 670
- 671
- 672
- 673
- 674
- 675
- 676